

# First-principles equations of state and elastic properties of seven metals

C. Bercegeay and S. Bernard

*Département de Physique Théorique et Appliquée, CEA-DIF, Boîte Postale 12, 91680 Bruyères-le-Châtel, France*

(Received 20 July 2005; revised manuscript received 23 September 2005; published 1 December 2005)

We present a systematic comparison of first-principles zero-temperature equations of state and elastic constants of seven metals (aluminum, titanium, copper, tantalum, tungsten, platinum, and gold) with the most recent diamond-anvil-cell (DAC) experimental data, for pressures up to 150 GPa. Our calculations were performed within density functional theory, testing both the local density approximation (LDA) and the generalized gradient approximation (GGA) to the exchange-correlation term, and using several types of pseudopotentials. The obtained pressure-volume relationships show good agreement with DAC data: the difference between *ab initio* pressure and experiment is at most 5 GPa at 100–150 GPa except for Au and Pt. The equilibrium volumes  $V_0$  and bulk moduli  $K_0$  are determined within 1.5% and 6% of DAC data respectively. Experimental results are better reproduced with GGA for Al, Ti, Cu, Ta and W, but with LDA for Pt and Au, in agreement with previous theoretical studies. The predicted elastic constants are within 10% of experiment. For tantalum we have also calculated phonon spectra under pressure. They are in excellent agreement with experimental data: especially they accurately reproduced the inflexion on the longitudinal branch in the  $\Gamma$ -H direction, which is typical of the VB column (V, Nb, Ta).

DOI: [10.1103/PhysRevB.72.214101](https://doi.org/10.1103/PhysRevB.72.214101)

PACS number(s): 64.30.+t, 71.15.Mb, 62.20.Dc

## I. INTRODUCTION

An important challenge for electronic-structure calculations is to predict the thermodynamic properties of matter [e.g., equations of state (EOS)] under extreme conditions outside the experimental domain. Such a predictivity is grounded on the ability of these calculations to reproduce all the experimental data to a good precision. Until recently, accurate experimental data were available from room pressure up to moderate pressures. With the development of sophisticated diamond-anvil cells (DACs), coupled to third-generation synchrotron sources, and the refinement of the corresponding pressure gauges, very accurate EOS data are now becoming available up to the megabar, and beyond.<sup>1</sup> We thus found it interesting to perform systematic calculations for a whole set of metals and to compare them to experimental data: not only EOS data, but also elastic constants at ambient conditions which are second-order derivatives of energy, and thus more sensitive to the quality of the calculations.

Seven metals were chosen: face-centered-cubic (fcc) Al, fcc Cu, body-centered-cubic (bcc) Ta, bcc W, fcc Pt and fcc Au, which do not show any phase transition up to 150 GPa at room temperature, and finally Ti which has a hexagonal-close-packed (hcp) structure at ambient conditions. At room temperature and under pressure (at 7.4 GPa,<sup>2</sup> 8 GPa,<sup>3</sup> or 9 GPa<sup>4,5</sup>), titanium is known to undergo a crystallographic phase change from hcp ( $\alpha$ ) into the  $\omega$  phase, which is a hexagonal lattice with three atoms per unit cell. The atomic positions are at (0,0,0),  $(1/3, 2/3, c/2a)$ , and  $(2/3, 1/3, c/2a)$ , where the  $c/a$  ratio is around 0.62. X-ray studies show that the  $\omega$  phase remains stable up to 87 GPa,<sup>3</sup> and 124–130 GPa.<sup>2</sup>

In the case of tantalum, for which an extensive set of theoretical calculations is available, we have also calculated phonon dispersion curves and phonon density of states from ambient pressure up to 1000 GPa.

We have chosen the plane-waves+pseudopotential (PP) formalism which is now widely used; moreover, each first-principles computer code usually provides built-in pseudopotentials. In this study, which initially was accompanying new experimental EOS measurements at high pressures, we have chosen to test these “ready-made” pseudopotentials, in order to evidence their possibilities, and also their limitations. For completeness, we compare our values to all-electron calculations available in the literature. The paper is organized as follows. In Sec. II the computational details are presented. In Sec. III and in Sec. IV we describe the procedure to determine the equilibrium lattice parameters and the elastic constants. In Sec. V we present briefly the calculation of phonon spectra. We summarize and discuss our results in Sec. VI, first for tantalum and then for the other six metals.

## II. COMPUTATIONAL DETAILS

Density-functional theory (DFT)<sup>6</sup> is a powerful tool for electronic structure calculations. It is generally assumed that in bulk solids, the local density approximation (LDA)<sup>7</sup> to the exchange-correlation term usually tends to underestimate the equilibrium lattice constants and to overestimate the bulk modulus, whereas the generalized gradient approximation (GGA)<sup>8</sup> overcompensates these errors and yields results closer to experiment.<sup>9</sup> But these are just general trends and as we shall see reality may be more complex. We thus performed total-energy calculations, both within LDA, using the Ceperley-Alder functional<sup>10</sup> as parametrized by Perdew and Wang, and GGA with the PW91 (Ref. 11) and PBE96 (Ref. 8) parametrizations. The choice of the exchange-correlation functional itself appears to be of second-order with respect to the LDA/GGA alternative.

A key issue in a pseudopotential is the number of so-called valence electrons, i.e., the electronic states which are explicitly taken into account in the calculation: even if this

TABLE I. Numerical parameters used for PP calculations. All pseudopotentials are HGH but PAW potentials for Al, Ti, and Cu (numbers in parentheses) and TM pseudopotentials for Pt (numbers in square brackets). Cutoff and smearing are given in Ry.

	Al	Ti	Cu	Ta	W	Pt	Au
Structure	fcc	hcp	fcc	bcc	bcc	fcc	fcc
Energy cutoff	(33)	(40)	200; (44)	40; 120 <sup>a</sup>	40; 100 <sup>a</sup>	[44]; 120	110
Irreducible $\mathbf{k}$ points	(56)	(252)	408; (120)	40	40	[60]; 60	28
Smearing	(0.01)	(0.01)	0.04; (0.01)	0.04	0.06	[0.04]; 0.04	0.04
Number of electrons	(3)	(12)	11; (17)	5; 13	6; 14	[10]; 18	11
Electronic states	$3s^2 3p^1$	$3s^2 3p^6 3d^2 4s^2$	$3p^6 3d^{10} 4s^1$	$5s^2 5p^6 5d^3 6s^2$	$5s^2 5p^6 5d^4 6s^2$	$[5d^9 6s^{0.95} 6p^{0.05}]$ ; $5s^2 5p^6 5d^{10}$	$5d^{10} 6s^1$

<sup>a</sup>Energy cutoff when semicore states are introduced.

separation appears quite naturally (the core states being usually well separated, both energetically and spatially from the valence states), in some cases, one has to take into account semicore states, in addition to the usual valence states. Once the valence states are chosen, several well-known mathematical formalisms can be used to generate the actual pseudopotential. In this study, we have used the separable “dual-space” Gaussian pseudopotentials of Hartwigsen, Goedecker and Hutter (HGH),<sup>12</sup> the norm-conserving Troullier-Martins (TM) pseudopotentials<sup>13</sup> from ABINIT package,<sup>14</sup> and projector augmented wave (PAW) potentials constructed by G. Kresse<sup>15</sup> and provided with the Vienna *Ab initio* Simulation Package (VASP).<sup>16</sup> Due to the poor quality of the existing pseudopotentials for platinum, we have generated a relativistic, norm-conserving TM pseudopotential for this element. It was constructed from a  $5d^9 6s^{0.95} 6p^{0.05}$  atomic configuration with cutoff radii of 2, 2.6, and 1.2 a.u. respectively.

Energy convergence tests were performed to determine the cutoff energy, the number of  $\mathbf{k}$  points, and the smearing for the Brillouin zone integration for each metal. The total energy was converged to 1 mRy per atom. Integration over the Brillouin zone was done using the special  $\mathbf{k}$ -point scheme of Monkhorst and Pack,<sup>17</sup> the  $\mathbf{k}$ -point sets were generated automatically. The determination of the elastic constants appears to require a stronger convergence in  $\mathbf{k}$  points, than the EOS calculation.<sup>18</sup> For example a  $12 \times 12 \times 12$  grid [which gives 112  $\mathbf{k}$  points in the irreducible Brillouin zone (IBZ) for a bcc lattice] leads to a convergence of  $2 \times 10^{-6}$  Ry for the energy in the EOS calculation. To calculate the  $C_{44}$  modulus of a cubic crystal a  $20 \times 20 \times 20$  grid (4200  $\mathbf{k}$  points in the IBZ) is needed to obtain the same convergence criterion. The electronic levels were populated according to the Methfessel and Paxton scheme.<sup>19</sup> All the technical data are listed in Table I.

### III. CALCULATION OF THE 0 K ISOTHERM

First we calculated the total energy for several values of the volume. Then the equations of state were determined by a least-squares fit of the total energy versus volume to the third-order Birch-Murnaghan equation,

$$E(V) = \sum_{n=0}^3 a_n V^{-2n/3}, \quad (1)$$

where  $V$  is the volume of the unit cell. The minimum-energy volume is found by minimizing (1), the bulk modulus

$K_0 = -V_0(dP/dV)_0$  is computed from the definition  $K(V) = V(d^2E/dV^2)$ , and its pressure derivative is defined by  $K'_0 = (dK/dP)_{P=0}$ . Pressure is written as in Ref. 20,

$$P = \frac{3}{2} K_0 \left[ \left( \frac{V_0}{V} \right)^{7/3} - \left( \frac{V_0}{V} \right)^{5/3} \right] \times \left\{ 1 + \frac{3}{4} (K'_0 - 4) \left[ \left( \frac{V_0}{V} \right)^{2/3} - 1 \right] \right\}. \quad (2)$$

For hcp structures, the  $c/a$  ratio has to be optimized at each volume. The optimization of the  $c/a$  ratio seems to have a small effect on the bulk modulus values.<sup>18</sup> This is the case here for hcp Ti: the optimized  $c/a$  value is 1.583 at the equilibrium volume, the experimental one is 1.588. The difference between these two values is less than 0.5%. The equilibrium volumes are the same and the bulk moduli differ by less than 1 GPa, which is within the error bar of the fitting procedure.

### IV. CALCULATION OF ELASTIC CONSTANTS

The elastic constants are obtained by straining the equilibrium lattice at fixed volumes, using volume-conserving strains and then computing the free energy as a function of strain. The lattice distortion transforms the primitive vectors  $a$  into the new vectors  $a'$

$$\overset{\leftrightarrow}{a}' = (\overset{\leftrightarrow}{I} + \overset{\leftrightarrow}{\epsilon}) \overset{\leftrightarrow}{a}, \quad (3)$$

where  $\overset{\leftrightarrow}{I}$  is the  $3 \times 3$  identity matrix and  $\overset{\leftrightarrow}{\epsilon}$  is a matrix containing the strain components

$$\overset{\leftrightarrow}{\epsilon} = \begin{pmatrix} \epsilon_{11} & \epsilon_{12} & \epsilon_{13} \\ \epsilon_{12} & \epsilon_{22} & \epsilon_{23} \\ \epsilon_{13} & \epsilon_{23} & \epsilon_{33} \end{pmatrix}. \quad (4)$$

#### A. Cubic crystals

The elastic behaviour of a cubic crystal is completely described by three independent constants  $C_{11}$ ,  $C_{12}$ , and  $C_{44}$ . The bulk modulus  $K$  is defined by a linear combination of the elastic constants

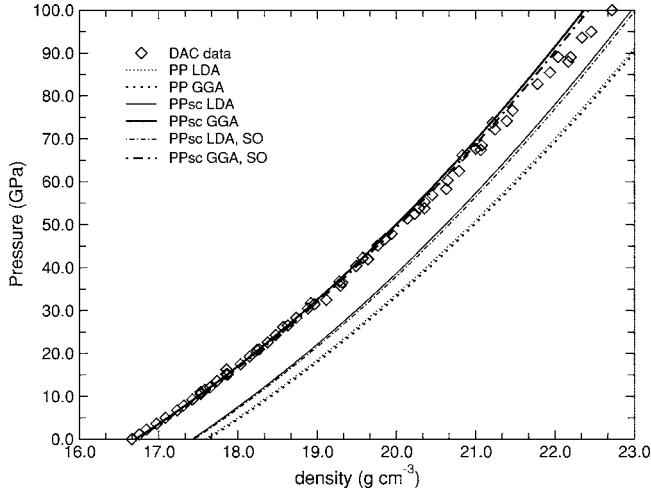


FIG. 1. Theoretical 0 K isotherm for bcc Ta compared with room temperature diamond-anvil-cell measurements (diamonds) (Ref. 1). Pseudopotentials used here are HGH with 5 (PP) or 13 (PPsc) valence electrons. In tantalum the “natural” five valence states are  $5d^36s^2$ . The introduction of the semicore states  $5s^25p^6$  (see Table I) improves the results.

$$K = \frac{C_{11} + 2C_{12}}{3}, \quad (5)$$

and was determined previously from the EOS using the Birch-Murnaghan fit, which allows us to compare both methods. The mechanical stability of the crystal implies that  $B$ ,  $C_{44}$ , and  $(C_{11} - C_{12})$  are all positive constants. To calculate  $C_{11} - C_{12}$ , we apply a tetragonal strain

$$\epsilon = \begin{pmatrix} \epsilon & 0 & 0 \\ 0 & \epsilon & 0 \\ 0 & 0 & (1 + \epsilon)^{-2} - 1 \end{pmatrix}, \quad (6)$$

where  $\epsilon$  is the magnitude of the strain. The corresponding strain energy is

$$F(\epsilon) = F(0) + 3(C_{11} - C_{12})V\epsilon^2 + O(\epsilon^3), \quad (7)$$

where  $F(0)$  is the free energy of the unstrained lattice and  $V$  its volume.  $C_{44}$  was obtained from a volume-conserving monoclinic strain<sup>21</sup>

$$\epsilon = \begin{pmatrix} 0 & \epsilon & 0 \\ \epsilon & 0 & 0 \\ 0 & 0 & \epsilon^2/(1 - \epsilon^2) \end{pmatrix}. \quad (8)$$

The corresponding strain energy is

$$F(\epsilon) = F(0) + 2C_{44}V\epsilon^2 + O(\epsilon^4). \quad (9)$$

We calculate the free energy for different strains, then we fit the points by a parabola, and the elastic constants are calculated from the quadratic coefficients.

### B. Hexagonal crystals

Hexagonal structures have five independent elastic constants:  $C_{11}$ ,  $C_{12}$ ,  $C_{13}$ ,  $C_{33}$ , and  $C_{44}$ . A sixth nonindependent

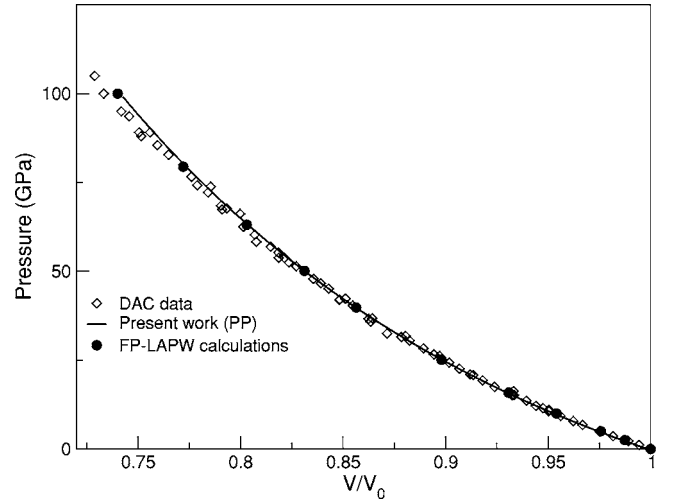


FIG. 2. Theoretical pressure versus relative volume for Ta (GGA). The white diamonds represent the DAC data from Ref. 1, the black circles are GGA results of Ref. 29 using the full-potential linearized augmented plane wave (FP-LAPW) method. The solid lines are present PP calculations.

constant  $C_{66}$  is equal to  $(C_{11} - C_{12})/2$ . The bulk modulus  $K$ , unlike the elastic constants  $C_{ij}$ , is given by a second derivative of the total energy per atom, but with respect to volume rather than strain. The bulk modulus is defined as<sup>18,22</sup>

$$K = \frac{2}{9}(C_{11} + C_{12} + 2C_{13} + C_{33}/2). \quad (10)$$

The mechanical stability conditions are  $C_{12}$ ,  $C_{33}$ ,  $C_{44}$ ,  $(C_{11} - C_{12})/2$ , and  $(C_{11} + C_{12} - 2C_{13}^2/C_{33})$ , all positive. The procedure to determine the elastic constants is the same as for cubic crystals. The complication with hcp crystals is that the unit cell is nonprimitive. The second basis atom (or *extra atom*) is free to move away from the position imposed by the homogeneous strain, so it must be relaxed independently. The five strains which are required can be found elsewhere.<sup>18</sup>

The calculations were done at the calculated equilibrium volume, which was constrained to be constant during the distortion, the  $c/a$  ratio being fixed at its experimental value. We only report unrelaxed constants for Ti, since relaxation, at room pressure, did not induce any noticeable variation of the elastic constants.

### V. PHONON CALCULATION

The calculation of full phonon dispersion curves and density of states under pressure is the next step towards a fully

TABLE II. EOS parameters for bcc Ta when the spin-orbit (SO) coupling is included or not.  $V_0$  are in  $\text{\AA}^3/\text{atom}$ ,  $K_0$  in GPa. The calculations are done with HGH pseudopotentials.

	LDA	LDA+SO	GGA	GGA+SO
$V_0$	17.27	17.25	18.04	17.99
$K_0$	217.44	215.45	195.58	196.84

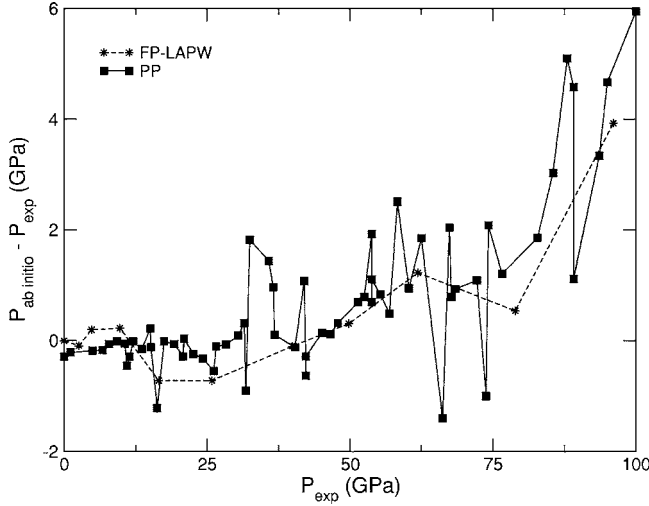


FIG. 3. Pressure difference between *ab initio* results and diamond-anvil-cell measurements versus experimental pressure for Ta. DAC data are from Dewaele *et al.* (Ref. 1). Filled black symbols are present pseudopotential calculations in GGA. Stars represent all-electron calculations in FP-LAPW, GGA performed by Wang *et al.* (Ref. 29).

*ab initio* thermal equation of state. In the framework of density functional perturbation theory (DFPT), the lattice distortion associated to a phonon is modeled as a perturbation to the electron density, which is calculated selfconsistently.<sup>23,24</sup> In practice, we calculate the full dynamical matrix on a mesh which spans the first Brillouin zone; all other frequencies are then deduced by a Fourier interpolation from this grid.<sup>24</sup> As for elastic constants, these calculations require an extremely strong convergence in  $\mathbf{k}$ -point sampling and are still CPU demanding. Yet they provide extremely rich information, which can be used for example to calculate a phonon Grüneisen coefficient, defined as the weighted average on all normal modes  $\mathbf{k},s$ , of the negative logarithmic derivative of the frequency  $\omega_s(k)$  of the mode with respect to volume. Following Ashcroft<sup>25</sup> we calculate, for a given volume  $V$ , the phonon Grüneisen parameter as

$$\gamma = \frac{\sum_{k,s} \gamma_{ks} c_{vs}(k)}{\sum_{k,s} c_{vs}(k)}, \quad (11)$$

where

$$c_{vs}(k) = \frac{\hbar \omega_s(k)}{V} \frac{\partial [e^{\beta \hbar \omega_s(k)} - 1]^{-1}}{\partial T} \quad (12)$$

is the contribution of the normal mode  $\mathbf{k},s$  to the specific heat and

$$\gamma_{ks} = - \frac{\partial [\ln \omega_s(k)]}{\partial \ln V}. \quad (13)$$

The summation spans the whole Brillouin zone. From our calculations of  $\omega_s(k)$  for discrete values of  $V$ , we perform a polynomial fit which we use to calculate  $\gamma_{ks}$ .

## VI. RESULTS AND DISCUSSIONS

### A. Tantalum

#### 1. Calculated equation of state

We present here the results of the full study performed for tantalum: 0 K isotherm, elastic constants, and phonon spectra. We compare our PP calculations with recent DAC data, where the maximal experimental pressures were 105 GPa for Ta.<sup>1</sup> The first-principles calculations were done at 0 K whereas DAC data were obtained for a temperature of 293 K. Yet, in this pressure range, the so-called thermal pressure is, according to our phonon calculations, between 0.5 and 1.5 GPa, and so it will be neglected.

In Fig. 1 we present all the results we obtained with different pseudopotentials where the number of valence electrons (with or without semicore states), the exchange-correlation functional (LDA or GGA), and the inclusion of spin-orbit coupling were tested. If we use the “natural” 5 valence electrons ( $5d^36s^2$ ), the equilibrium volume is wrong by 5%, both for LDA and GGA. If we include the  $5s$  and  $5p$  semicore states in the valence, then  $V_0$  within LDA is slightly better, whereas within GGA, the agreement with experiment is perfect.

Spin-orbit coupling is found to have a small effect on the values of  $V_0$  and  $K_0$ , both within LDA and GGA. The values obtained for  $V_0$  and  $K_0$  with and without spin-orbit coupling are listed in Table II, for a given class of pseudopotentials (i.e., HGH).

Introducing spin-orbit coupling leads to  $\Delta V_0 \approx 0.2\%$  and  $\Delta K_0 \approx 1\%$  for Ta. It is in agreement with previous studies<sup>26,27</sup> and in slight contradiction with Söderlind *et al.*<sup>28</sup> We thus did not include spin-orbit coupling in further calculations.

EOS results for Ta are summarized in Table III. GGA appears to give the best results, which agrees with all-

TABLE III. Zero-pressure properties of tantalum obtained with pseudopotential calculations from a Birch-Murnaghan fit. Lattice parameters  $a_0$  are given in Å, equilibrium volumes  $V_0$  in Å<sup>3</sup>/atom, bulk moduli  $K_0$  in GPa. DAC data are from Dewaele *et al.* (Ref. 1) and previous all-electron studies are from Boettger (Ref. 26). The best results are in bold.

PP	Present work				DAC data			Previous all-electron works				
		$a_0$	$V_0$	$K_0$	$K'_0$	$V_0$	$K_0$	$K'_0$		$V_0$	$K_0$	
HGH	LDA	3.26	17.27	217.44	3.71	18.04	194	3.52	LCGTO-FF	LDA	17.35	209
<b>HGH</b>	<b>GGA</b>	<b>3.3</b>	<b>18.04</b>	<b>195.58</b>	<b>3.67</b>				LCGTO-FF	GGA	18.35	190

electron studies of Boettger.<sup>26</sup> Equilibrium volumes obtained with pseudopotentials are globally lower than all-electron results by 0.5% to 1.7%, for LDA and GGA respectively. Bulk moduli determined by PP calculations are rather greater than those deduced from all-electron methods by 3–4%. The equilibrium volume and the bulk modulus obtained from PP calculations agree very well with the DAC results.

We have plotted in Fig. 2 pressure versus volume compression  $V/V_0$ , where  $V_0$  is the theoretical equilibrium volume for first-principles calculations and the experimental one for DAC data. We can see that there is a very good reproduction of the DAC data up to  $\approx 100$  GPa. This trend is evidenced on Fig. 3 where we have plotted the pressure difference between *ab initio* results and DAC data versus the experimental pressure for PP calculations. The difference between theoretical and experimental pressures does not exceed 6 GPa for Ta, at 100 GPa. It is in agreement with LAPW calculations of Wang *et al.*<sup>29</sup>

## 2. Calculated elastic constants

In Table IV the calculated and experimental values of the elastic constants for tantalum are listed. They were calculated at the theoretical equilibrium volumes, using our best pseudopotential. When comparing the theoretical and experimental elastic constants, we see that the deviations vary between 3% and 22%, the worst agreement being found for  $C_{44}$ . Gülsiren and Cohen<sup>30</sup> found that thermal effects at constant volume are quite small except at pressures greater than 200 GPa, and that  $C_{44}$  tends to soften at zero pressure with increasing temperature. So our results should not be improved by adding temperature effects.

## 3. Phonon spectra in tantalum under pressure

The calculations were performed using the HGH pseudo-potential within GGA and without spin-orbit coupling (we checked that the influence of spin-orbit coupling was negli-

TABLE IV. Elastic constants at 0 K (in GPa) for bcc Ta.  $(C_{11}-C_{12})/2$  and  $K$  are added for comparison.  $K$  is calculated by Eq. (5).

	$C_{11}$	$C_{12}$	$C_{44}$	$\frac{C_{11}-C_{12}}{2}$	$K$
Present	258.7	168.8	67.8	45	198.8
exp. <sup>a</sup>	266.3	158.2	87.4	54.1	194.2
exp. <sup>b</sup>	266	161	82.5	52.5	196

<sup>a</sup>Reference 31.

<sup>b</sup>Reference 32.

gible). We calculated the full dynamical matrix on an  $8 \times 8 \times 8$  grid in the full Brillouin zone, which amounts to 29 inequivalent  $\mathbf{q}$  vectors in the irreducible BZ. The dispersion curves along symmetry directions and the phonon density of states were then calculated by a Fourier interpolation on this grid. The whole process was iterated for six values of the atomic volume, corresponding to pressures from 0 to 1000 GPa.

On Fig. 4 we plot the phonon dispersion curves that we have calculated at ambient pressure along high symmetry directions in reciprocal space. They are in excellent agreement with the inelastic neutron diffraction data of Woods.<sup>33</sup> Especially, the inflexion on the longitudinal branch in the  $\Gamma$ -H direction, which is typical of the VB column (V, Nb, Ta) is accurately reproduced. These anomalies tend to disappear under pressure, giving dispersion curves typical of normal bcc elements, as can be seen on Fig. 5. From the calculated phonon density of states at various atomic volumes, it is possible, by an averaging procedure, to calculate the evolution of the phonon Grüneisen parameter under pressure.

In Fig. 6 we can see that our calculations are consistent with other theoretical approaches, even if we predict a slightly different decrease with increasing pressure.<sup>28,34</sup> Yet it can be noticed that there is a wide dispersion of the calculated values.

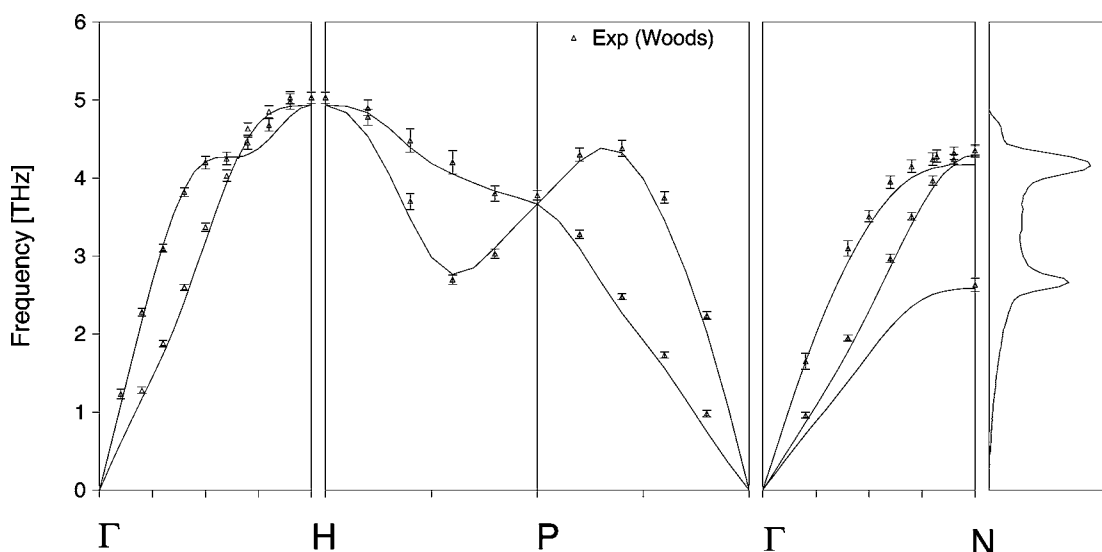


FIG. 4.  $P=0$  phonon dispersion curves for Ta and phonon density of states (extreme right), compared to the inelastic neutron diffraction data of Woods (Ref. 33).

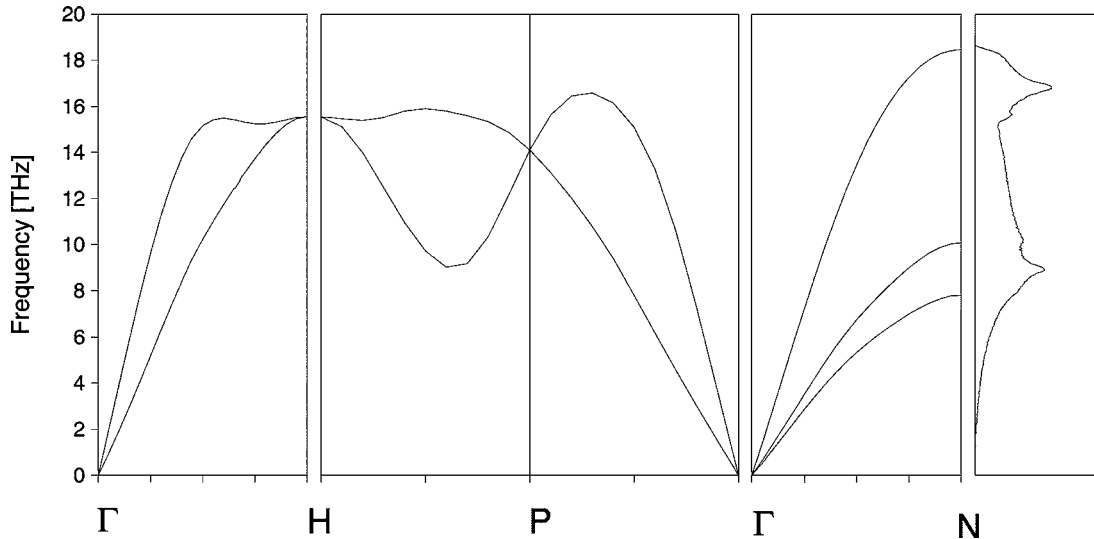


FIG. 5.  $P=1000$  GPa phonon dispersion curves for Ta and phonon density of states (extreme right).

## B. Al, Ti, Cu, W, Pt, Au

### 1. Equations of state

Given our accurate results concerning EOS and elastic constants for Ta, we chose to test pseudopotentials and the exchange-correlation functional on six other metals: Al, Ti, Cu, W, Pt, and Au. For each metal we calculated equation of state up to 150 GPa and elastic constants, and systematically compared our PP calculations with recent DAC data. The maximal experimental pressures were 94 GPa for Au and Pt, and 153 GPa for Cu, Al, and W.<sup>1</sup> The thermal pressures were estimated according to 0 K and 293 K isotherms, in Refs. 35–37 to be less than 1.7 GPa for the six metals, and as for Ta was neglected.

The general trend that  $V_0$  within GGA is slightly better than within LDA was also observed for Al, Ti, Cu, and W, yet it does not seem to be true for platinum. However, if one only includes  $5d$  and  $6s$  electrons in the valence, the equilibrium properties are slightly improved. This could be related to the fact that, at the atomic level, the  $4f$  states are very close in energy to the  $5s$  states; so, if one includes the  $5s$  and  $5p$  states in the valence, one should also treat the  $4f$  states on an equal footing.

Spin-orbit coupling is found to have a small effect on the values of  $V_0$  and  $K_0$ , both within LDA and GGA. We tested its effect on the EOS for the other three heavy metals, W, Pt, and Au. The values obtained for  $V_0$  and  $K_0$  with and without spin-orbit coupling are listed in Table V, for HGH pseudopotentials.

Introducing spin-orbit coupling leads to  $\Delta V_0 \approx 0.2\%$ ,  $\Delta K_0 \approx 2\%$  for W, and  $\Delta V_0 \leq 1\%$ ,  $\Delta K_0 \leq 5\%$  for Pt and Au. It is in agreement with previous studies on gold.<sup>43</sup> We thus did not include spin-orbit coupling in further calculations, except for the TM pseudopotential for platinum. Maybe a full treatment of relativistic effects would be necessary to unambiguously quantify this effect.

All our EOS results are summarized in Table VI. GGA appears to be the best exchange-correlation approximation for Al, Ti, Cu, and W, which agrees with all-electron studies

of Ostanin *et al.*<sup>40</sup> and Jona *et al.*<sup>41</sup> on titanium and copper respectively. On the contrary, LDA is found to give better results for Pt and Au. Boettger<sup>43</sup> has already found that LDA predicts  $V_0$  and  $K_0$  correctly for gold. Equilibrium volumes obtained with pseudopotentials are globally lower than all-electron results by less than 1.5%. On the contrary, bulk moduli determined by PP calculations are greater than those deduced from all-electron methods by less than 9%. Such a dispersion appears to be normal, as bulk moduli are deduced from analytical fits of raw *ab initio* data. The equilibrium volume is determined within less than 1.5% of experiment except for Ti, the error on bulk modulus is within 6% except for Ti and Au. So our global results compare well with experimental and all-electron data, showing the good accuracy of the pseudopotentials used here.

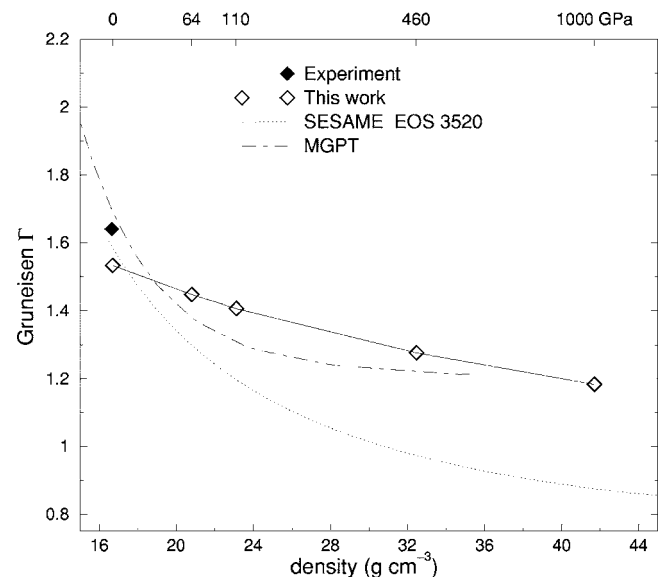


FIG. 6. Calculated evolution of the Grüneisen parameter with density for Ta and comparison with other approaches. The corresponding pressures can be found on the upper horizontal axis.

TABLE V. EOS parameters for W, Pt, and Au when the spin-orbit (SO) coupling is included or not.  $V_0$  are in  $\text{\AA}^3/\text{atom}$ ,  $K_0$  in GPa. The calculations are done with HGH pseudopotentials.

	LDA	LDA+SO	GGA	GGA+SO
<b>W bcc</b>				
$V_0$	15.45	15.48	15.95	15.99
$K_0$	338.01	330.28	309.96	304.06
<b>Pt fcc</b>				
$V_0$	14.82	14.9	15.59	15.74
$K_0$	305.99	297.01	250.85	241.81
<b>Au fcc</b>				
$V_0$	17.06	16.91	18.13	17.9
$K_0$	181.98	188.95	135.13	142.25

We have plotted in Figs. 7 and 8 pressure versus the volume compression  $V/V_0$ . We can see that for Al, Cu, and W there is a very good reproduction of the DAC data up to 150 GPa. This trend is evidenced on Fig. 9 where the difference between theoretical and experimental pressures does not exceed 6 GPa for these three metals. It is in agreement with LAPW calculations of Wang *et al.*<sup>29</sup>

As for Au and Pt, not only do we obtain poor equilibrium properties, but we also find a systematic increase with pressure, the deviation between theory and experiment reaching 8 GPa near 100 GPa. It confirms the fact that in our calculations, we miss part of the physics specific to these two

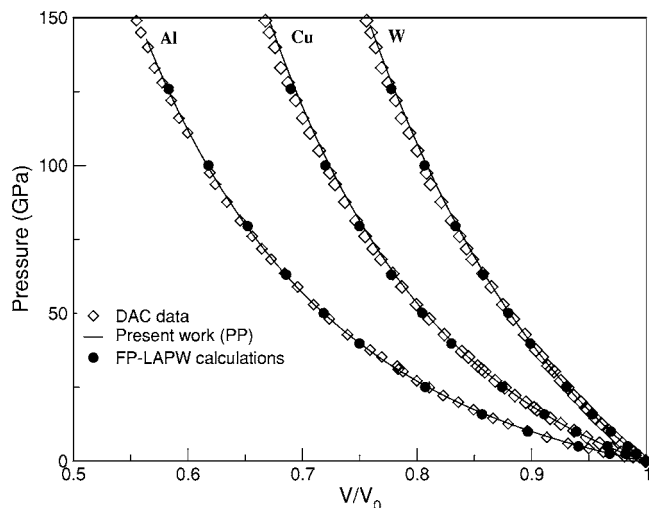


FIG. 7. Theoretical pressure versus relative volume for Al, Cu, and W (GGA). The white diamonds represent the DAC data from Ref. 1, the black circles are FP-LAPW (GGA) results of Ref. 29. The solid lines are present PP calculations.

elements. The same trend should also occur for  $\omega$ -Ti.

## 2. Elastic constants

Given the poor quality of our EOS results for Au and Pt, it was useless to calculate their elastic constants. So we restricted ourselves to the four other metals (Al, Cu, Ti, and W) and in the case of Ti we consider only the hcp phase. In

TABLE VI. Zero-pressure properties of all the studied metals (for Ta see Table III) obtained with pseudopotential calculations from a Birch-Murnaghan fit. Lattice parameters  $a_0$  are given in  $\text{\AA}$ , equilibrium volumes  $V_0$  in  $\text{\AA}^3/\text{atom}$ , bulk moduli  $K_0$  in GPa. DAC data are from Dewaele *et al.* (Ref. 1) except for Ti (see Ref. 38). The best results are in bold.

Metal	Present work						DAC data			Previous all-electron works						
	PP	$a_0$	$V_0$	$K_0$	$K'_0$		$V_0$	$K_0$	$K'_0$		$V_0$	$K_0$	Ref.			
Al	LDA	PAW	3.98	15.81	83.5	4.59	16.57	73	4.54	GTO <sup>a</sup>	LDA	15.85	82.85	39		
		<b>GGA</b>	<b>PAW</b>	<b>4.05</b>	<b>16.58</b>	<b>77.36</b>					<b>4.23</b>	GTO	GGA	16.51	74.12	39
Ti hcp	LDA	PAW	2.86	16.09	130.04	3.01	17.7	117	3.9	FP-LMTO <sup>b</sup>	GGA	17.36	114	40		
		<b>GGA</b>	<b>PAW</b>	<b>2.93</b>	<b>17.31</b>	<b>112.47</b>					<b>3.59</b>					
Ti $\omega$	<b>GGA</b>	<b>PAW</b>	<b>3.71</b>	<b>17.08</b>	<b>114.23</b>	<b>3.46</b>	17.4	138	3.8							
Cu	LDA	HGH	3.54	11.09	178.62	4.95	11.81	133	5.3	FP-LAPW <sup>c</sup>	LDA	11.26	177.7	41		
		GGA	HGH	3.64	12.05	134.19					4.94	FP-LAPW	GGA	12	148.7	41
		<b>GGA</b>	<b>PAW</b>	<b>3.63</b>	<b>11.99</b>	<b>138.47</b>					<b>4.97</b>					
W	LDA	HGH	3.14	15.45	338.01	4.35	15.86	296	4.3	LAPW <sup>d</sup>	LDA	15.51	337	9		
		<b>GGA</b>	<b>HGH</b>	<b>3.17</b>	<b>15.95</b>	<b>309.96</b>					<b>4</b>	LAPW	GGA	16.15	307	9
Pt	LDA	HGH	3.9	14.82	305.99	5.32	15.1	277	5.08	FP-LMTO	LDA	14.9	280.8	42		
		GGA	HGH	3.97	15.59	250.85					5.65					
Au	<b>LDA</b>	<b>HGH</b>	<b>4.09</b>	<b>17.06</b>	<b>181.98</b>	<b>5.77</b>	16.96	167	6	LCGTO-FF <sup>e</sup>	LDA	16.48	190	43		
		GGA	HGH	4.17	18.13	135.13					6	LCGTO-FF	GGA	17.89	142	43

<sup>a</sup>GTO: Gaussian-type orbitals.

<sup>b</sup>FP-LMTO: Full-potential linear muffin-tin orbital.

<sup>c</sup>FP-LAPW: Full-potential linearized augmented plane wave.

<sup>d</sup>LAPW: Linearized augmented plane wave.

<sup>e</sup>LCGTO-FF: Linear combinations of Gaussian-type orbitals fitting function.

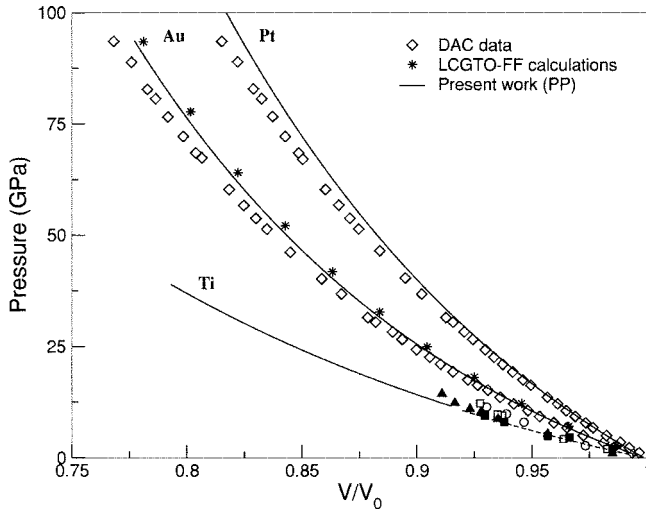


FIG. 8. Theoretical pressure versus relative volume for Au, Pt (LDA), and Ti (GGA). The diamonds represent the DAC data from Ref. 1. Other symbols correspond to experiments carried out under different pressure media as in Fig. 7 of Ref. 38. The stars are LDA calculations of Ref. 43, using linear combinations of Gaussian-type orbitals fitting function (LCGTO-FF) method. The solid (Au, Pt,  $\omega$ -Ti) and dashed lines (hcp Ti) are present work.

Table VII the calculated values of the elastic constants are listed and compared to experiment. They were calculated at the theoretical equilibrium volumes, using our best pseudopotential for each element. When comparing the theoretical and experimental elastic constants, we see that generally the

TABLE VII. Elastic constants at 0 K (in GPa) for cubic (Al, Cu, W) and hexagonal (Ti) metals. The elastic constants of Ti are unrelaxed.  $K$  is calculated by Eq. (5) for cubic structures and Eq. (10) for hcp ones.  $(C_{11}-C_{12})/2$  and  $K$  are added for comparison.

		$C_{11}$	$C_{12}$	$C_{44}$	$\frac{C_{11}-C_{12}}{2}$	$K$	$C_{13}$	$C_{33}$
<b>Al</b>	Present	108.2	56.6	30.5	25.8	73.8	-	-
	exp. <sup>a</sup>	123	70.8	30.9	26.1	88.2	-	-
	exp. <sup>b</sup>	114.3	61.9	31.6	26.2	79.4	-	-
	exp. <sup>c</sup>	106.8	60.4	28.3	23.2	75.9	-	-
<b>Cu</b>	Present	171.1	122.2	75.3	24.5	138.5	-	-
	exp. <sup>d</sup>	176.2	124.9	81.8	25.7	142	-	-
	exp. <sup>e</sup>	166.1	119.9	75.6	23.1	135.3	-	-
<b>W</b>	Present	502.6	213.6	145.9	144.5	309.9	-	-
	exp. <sup>f</sup>	532.6	205	163.1	163.8	314.2	-	-
<b>Ti</b>	Present	171.6	85	39	43.3	112.8	78.6	187.5
	exp. <sup>g</sup>	176.1	86.9	50.8	44.6	110	68.3	190.5

<sup>a</sup>Reference 44.

<sup>b</sup>Reference 45.

<sup>c</sup>Reference 46

<sup>d</sup>Reference 47.

<sup>e</sup>Reference 48.

<sup>f</sup>Reference 31.

<sup>g</sup>Reference 49.

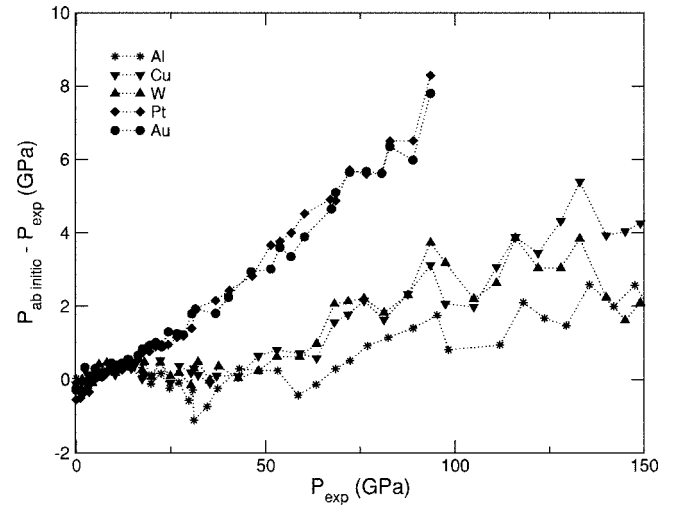


FIG. 9. Pressure difference between *ab initio* results and diamond-anvil-cell measurements versus experimental pressure. DAC data are from Dewaele *et al.* (Ref. 1). Filled black symbols are present pseudopotential calculations in LDA (Pt, Au) or GGA (Al, Cu, W).

discrepancy is less than 10% but can reach  $-23\%$  and  $+16\%$  in the worst cases ( $C_{44}$  and  $C_{13}$  for Ti). This range is comparable with previous studies.

## VII. CONCLUSION

We have performed extensive calculations of equations of state under pressure on seven metals using various available pseudopotentials. In most cases, we obtain a fair agreement with recent high pressure DAC measurements, usually better than 5 GPa up to 150 GPa. The present calculations compare also well with previous all-electron studies, and give the same trend with respect to experiment as for LDA/GGA approximations. The generalized gradient approximation appears to give best equilibrium properties for all metals except for Au and Pt where local density approximation is better, which remains to be explained, beyond error compensations.

The elastic constants are determined within 10–20% of experiment. This deviation range corresponds to a typical order of magnitude for the precision obtained in other studies on these quantities, which are extremely sensitive to the convergence of the calculation, apart from the quality of the pseudopotential itself.

So this work gives a wide range of data of static and elastic properties for different metals, which reproduce the experimental data quite well. It encourages further studies with pseudopotential methods for the prediction of properties where no experimental data are available.

However, the true challenge now for first-principles calculations is to predict temperature properties with good accuracy, in order to calculate fully *ab initio* equations of state. One first step towards this goal is to calculate *ab initio* phonon spectra. In this paper we have presented our results for

tantalum from ambient up to 1000 GPa pressures. From these calculations, we have deduced a Grüneisen coefficient versus density, which is a building block for full domain equation of state construction.

## ACKNOWLEDGMENTS

We acknowledge Pierre-Matthieu Anglade, Agnès Dewaele, and Paul Loubeyre for fruitful discussions.

- <sup>1</sup>A. Dewaele, P. Loubeyre, and M. Mezouar, *Phys. Rev. B* **70**, 094112 (2004). For all metals a Vinet formulation was used to fit the  $P(V)$  data. In these experiments, helium was the pressure transmitting medium, which leads to quasihydrostatic conditions. The bulk modulus was fixed to its ultrasonic value during the EOS fit.
- <sup>2</sup>Y. Akahama, H. Kawamura, and T. Le Bihan, *Phys. Rev. Lett.* **87**, 275503 (2001).
- <sup>3</sup>H. Xia, G. Parthasarathy, H. Luo, Y. K. Vohra, and A. L. Ruoff, *Phys. Rev. B* **42**, 6736 (1990).
- <sup>4</sup>Y. K. Vohra and P. T. Spencer, *Phys. Rev. Lett.* **86**, 3068 (2001).
- <sup>5</sup>R. Ahuja, L. Dubrovinsky, N. Dubrovinskaia, J. M. Osorio Guillen, M. Mattesini, B. Johansson, and T. Le Bihan, *Phys. Rev. B* **69**, 184102 (2004).
- <sup>6</sup>P. Hohenberg and W. Kohn, *Phys. Rev.* **136**, B864 (1964).
- <sup>7</sup>W. Kohn and L. J. Sham, *Phys. Rev.* **140**, A1133 (1965).
- <sup>8</sup>J. P. Perdew, K. Burke, and M. Ernzerhof, *Phys. Rev. Lett.* **77**, 3865 (1996).
- <sup>9</sup>A. Khein, D. J. Singh, and C. J. Umrigar, *Phys. Rev. B* **51**, 4105 (1995).
- <sup>10</sup>D. M. Ceperley and B. J. Alder, *Phys. Rev. Lett.* **45**, 566 (1980).
- <sup>11</sup>J. P. Perdew, J. A. Chevary, S. H. Vosko, K. A. Jackson, M. R. Pederson, D. J. Singh, and C. Fiolhais, *Phys. Rev. B* **46**, 6671 (1992).
- <sup>12</sup>C. Hartwigsen, S. Goedecker, and J. Hutter, *Phys. Rev. B* **58**, 3641 (1998).
- <sup>13</sup>N. Troullier and J. L. Martins, *Phys. Rev. B* **43**, 1993 (1991).
- <sup>14</sup>X. Gonze, J.-M. Beuken, R. Caracas, F. Detraux, M. Fuchs, G.-M. Rignanese, L. Sindic, M. Verstraete, G. Zerah, F. Jollet, M. Torrent, A. Roy, M. Mikani, Ph. Ghosez, J.-Y. Raty, and D. C. Allan, *Comput. Mater. Sci.* **25**, 478 (2002), ABINIT is a common project of the Université Catholique de Louvain, Corning Incorporated, and other contributors (<http://www.abinit.org>).
- <sup>15</sup>G. Kresse and D. Joubert, *Phys. Rev. B* **59**, 1758 (1999).
- <sup>16</sup>G. Kresse and J. Furthmüller, *Comput. Mater. Sci.* **6**, 15 (1996).
- <sup>17</sup>H. J. Monkhorst and J. D. Pack, *Phys. Rev. B* **13**, 5188 (1976).
- <sup>18</sup>L. Fast, J. M. Wills, B. Johansson, and O. Eriksson, *Phys. Rev. B* **51**, 17431 (1995).
- <sup>19</sup>M. Methfessel and A. T. Paxton, *Phys. Rev. B* **40**, 3616 (1989).
- <sup>20</sup>J.-P. Poirier, *Introduction to the Physics of the Earth's Interior* (Cambridge University Press, Cambridge, 1991), p. 64.
- <sup>21</sup>M. J. Mehl, B. M. Klein, and D. A. Papaconstantopoulos, in *Intermetallic Compounds: Principles and Practice*, edited by J. H. Westbrook and R. L. Fleischer (Wiley, New York, 1993), Vol. I, Chap. 9, pp. 195–210.
- <sup>22</sup>S. L. Qiu and P. M. Marcus, *Phys. Rev. B* **68**, 054103 (2003).
- Following Qiu and Marcus, if in the calculation the  $c/a$  ratio is kept constant while the volume changes, a constrained bulk modulus  $K^{(c)}$  is defined as:  $K^{(c)} = \frac{2}{9}(C_{11} + C_{12} + 2C_{13} + C_{33}/2)$ . If  $c/a$  is allowed to change with the volume, the bulk modulus should be calculated as  $K = [C_{33}(C_{11} + C_{12}) - 2C_{13}^2](C_{11} + C_{12} + 2C_{33} - 4C_{13})$ . It can be noticed that since  $C_{11} + C_{12}$ ,  $C_{13}$ , and  $C_{33}$  are not affected by the internal relaxation, there is no internal relaxation effect on either  $K^{(c)}$  or  $K$ .
- <sup>23</sup>X. Gonze, *Phys. Rev. B* **55**, 10337 (1997).
- <sup>24</sup>X. Gonze and C. Lee, *Phys. Rev. B* **55**, 10355 (1997).
- <sup>25</sup>N. W. Ashcroft and D. A. Mermin, *Solid State Physics* (HRW International Editions, New York, 1976), pp. 492–493.
- <sup>26</sup>J. C. Boettger, *Phys. Rev. B* **64**, 035103 (2001).
- <sup>27</sup>R. E. Cohen and O. Gülseren, *Phys. Rev. B* **63**, 224101 (2001).
- <sup>28</sup>P. Söderlind and J. A. Moriarty, *Phys. Rev. B* **57**, 10340 (1998).
- <sup>29</sup>Y. Wang, D. Chen, and X. Zhang, *Phys. Rev. Lett.* **84**, 3220 (2000).
- <sup>30</sup>O. Gülseren and R. E. Cohen, *Phys. Rev. B* **65**, 064103 (2002).
- <sup>31</sup>F. H. Featherston and J. R. Neighbours, *Phys. Rev.* **130**, 1324 (1963).
- <sup>32</sup>K. W. Katahara, M. H. Manghnani, and E. S. Fisher, *J. Appl. Phys.* **47**, 434 (1976).
- <sup>33</sup>A. D. B. Woods, *Phys. Rev.* **136**, A781 (1964).
- <sup>34</sup>J. A. Moriarty, J. F. Belak, R. E. Rudd, P. Söderlind, F. H. Streitz, and L. H. Yang, *J. Phys.: Condens. Matter* **14**, 2825 (2002).
- <sup>35</sup>R. McQueen, S. Marsh, J. Taylor, J. Fritz, and W. Carter, *High Velocity Impact Phenomena* (Academic, New York, 1970), pp. 531–543.
- <sup>36</sup>J. A. Morgan, *High Temp. - High Press.* **6**, 195 (1974).
- <sup>37</sup>O. L. Anderson, D. G. Isaak, and S. Yamamoto, *J. Appl. Phys.* **65**, 1534 (1989).
- <sup>38</sup>D. Errandonea, Y. Meng, M. Somayazulu, and D. Häusermann, *Physica B* **355**, 116 (2004).
- <sup>39</sup>J. E. Jaffe, R. J. Kurtz, and M. Gutowski, *Comput. Mater. Sci.* **18**, 199 (2000).
- <sup>40</sup>S. A. Ostanin and V. Y. Trubitsin, *J. Phys.: Condens. Matter* **9**, L491 (1997).
- <sup>41</sup>F. Jona and P. M. Marcus, *Phys. Rev. B* **63**, 094113 (2001).
- <sup>42</sup>T. Tsuchiya and K. Kawamura, *Phys. Rev. B* **66**, 094115 (2002).
- <sup>43</sup>J. C. Boettger, *Phys. Rev. B* **67**, 174107 (2003).
- <sup>44</sup>P. M. Sutton, *Phys. Rev.* **91**, 816 (1953).
- <sup>45</sup>G. N. Kamm and G. A. Alers, *J. Appl. Phys.* **35**, 327 (1964).
- <sup>46</sup>J. J. F. Thomas, *Phys. Rev.* **175**, 955 (1968).
- <sup>47</sup>J. W. C. Overton and J. Gaffney, *Phys. Rev.* **98**, 969 (1955).
- <sup>48</sup>Y. Hiki and A. V. Granato, *Phys. Rev.* **144**, 411 (1966).
- <sup>49</sup>E. S. Fisher and C. J. Renken, *Phys. Rev.* **135**, A482 (1964).